Supporting information

Nanoparticle-based Tough Polymers with Crack-propagation Resistance

Yuma Sasaki,[1] Yuichiro Nishizawa,[1] Takumi Watanabe,[1] Takuma Kureha,[3] Kazuya Uenishi,[4] Kazuko Nakazono,[5] Toshikazu Takata,*[5,6] and Daisuke Suzuki*[1,2]

[1]Graduate School of Textile Science & Technology, Shinshu University, 3-15-1 Tokida, Ueda, Nagano 386-8567, Japan

[2]Research Initiative for Supra-Materials, Interdisciplinary Cluster for Cutting Edge Research, Shinshu University, 3-15-1 Tokida, Ueda, Nagano 386-8567, Japan

[3]Department of Frontier Materials Chemistry, Graduate School of Science and Technology, Hirosaki University, 3 Bunkyo-cho, Hirosaki 036-8561, Japan

[4]Yokohama Rubber Co., Ltd., 2-1 Oiwake, Hiratsuka, Kanagawa 254-8601, Japan.

[5]Department of Chemical Science and Engineering, Tokyo Institute of Technology, 4259 Nagatsuta-cho, Midori-ku, Yokohama, Kanagawa 226-8503, Japan

[6]Graduate School of Advanced Science and Engineering, Hiroshima University, 1-4-1 Kagamiyama, Higashi-Hiroshima, Hiroshima 739-8527, Japan

Experimental Details

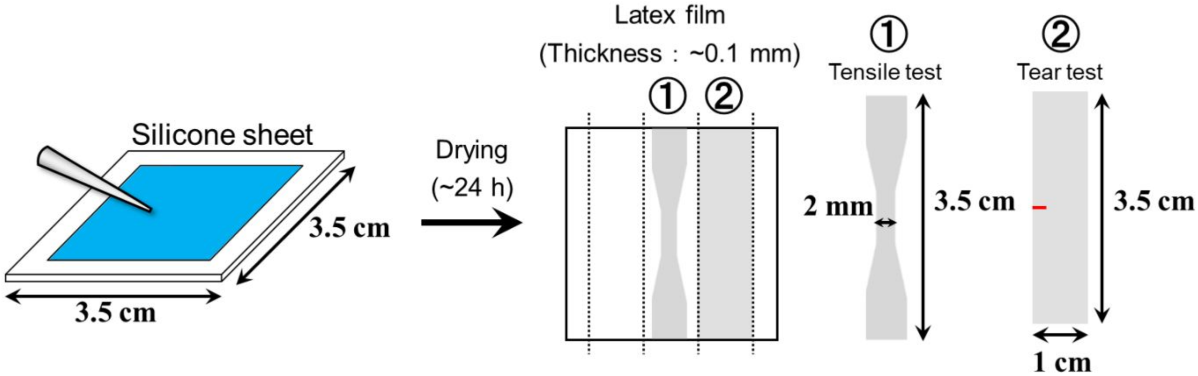

Figure S1. Schematic illustration of the preparation of the tear test specimens.

Results and Discussion

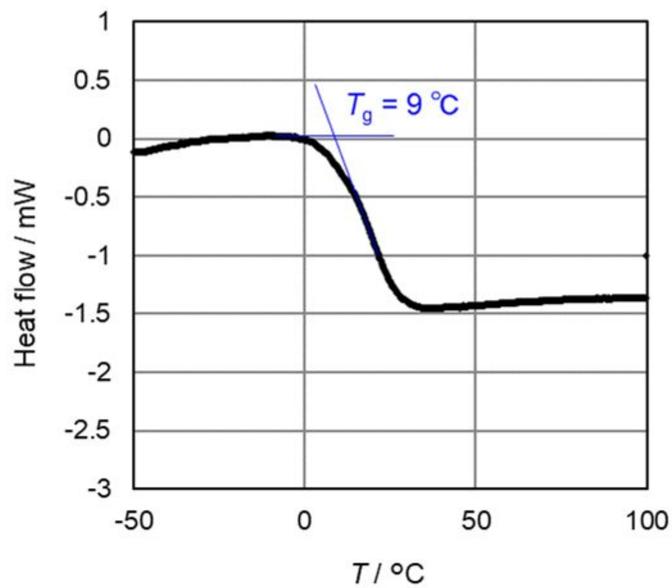

Figure S2. Representative DSC curve (second heating) for an EM microparticle at a heating rate of 10 °C/min. T_g was calculated from the cross-point of tangents to the baseline and inflection point.

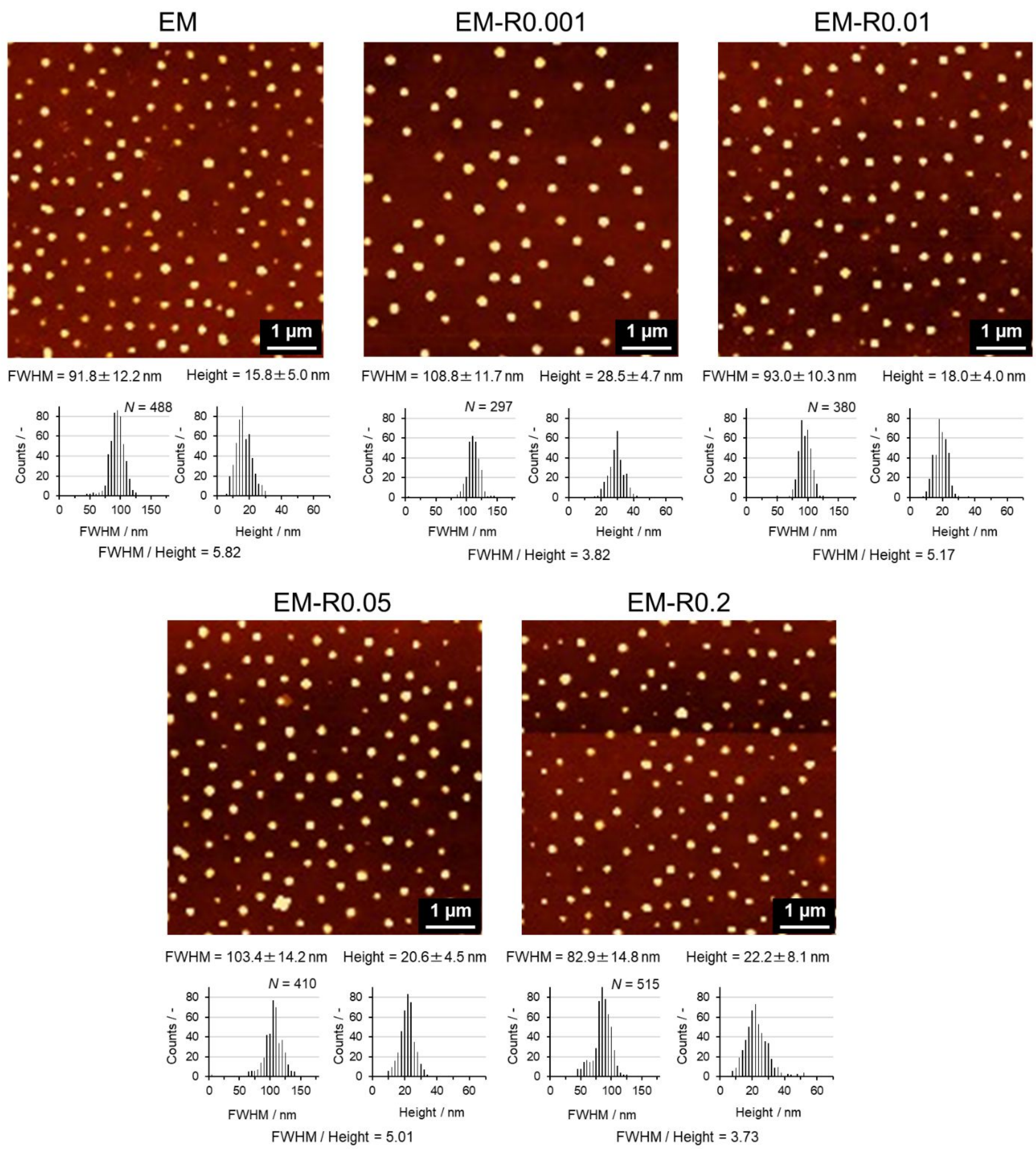

Figure S3. AFM height images of the EM and EM-RX (X = 0.001, 0.01, 0.05, 0.2) microparticles dried on a glass substrate and their determined sizes (FWHM and the maximum height).

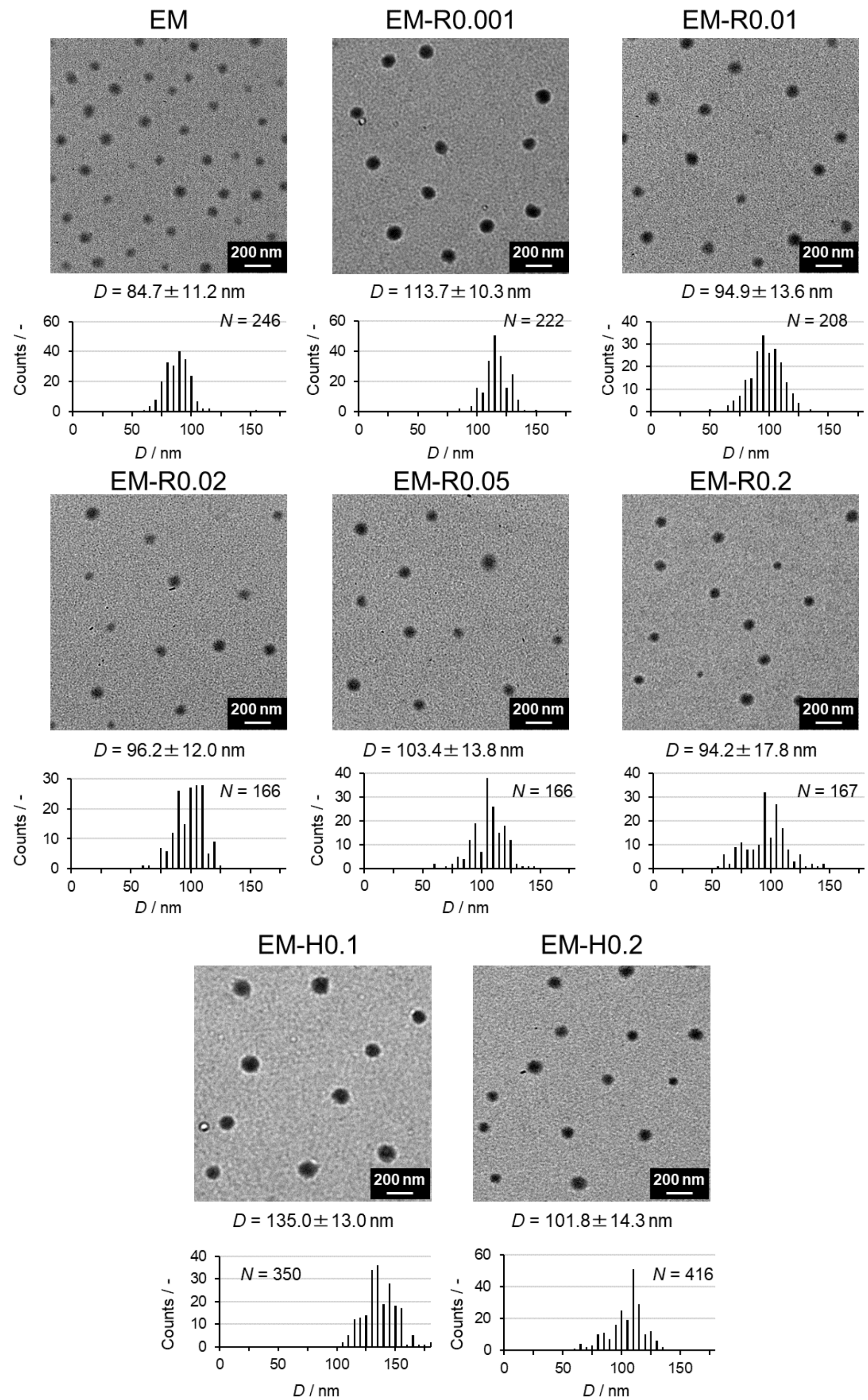

Figure S4. TEM images of EM and EM-R*X* (*X* = 0.001, 0.01, 0.02, 0.05, 0.2) as well as EM-H*Y* (*Y* = 0.1, 0.2) microparticles dried on the copper grid.

(a)

	Mass of soluble fraction w_1 / mg	Original mass w_2 / mg	GC% $= (w_2 - w_1) / w_2 \times 100$
EM	614.9	619.6	<1
EM-R0.001	598.0	602.8	<1
EM-R0.01	601.8	620.8	3
EM-R0.02	270.7	285.0	5
EM-R0.05	473.4	592.3	20
EM-R0.2	476.9	768.3	38

(b)

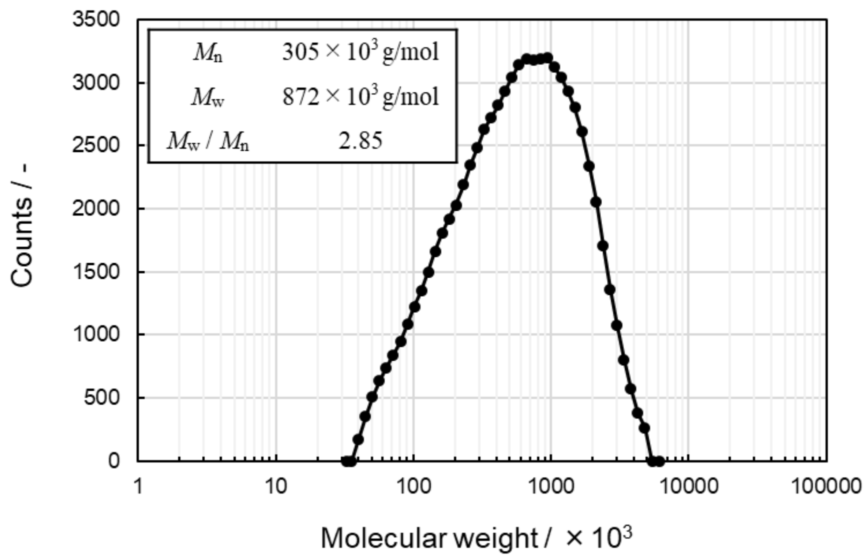

Figure S5 (a) Weight of the soluble mass (w_1) and original mass (w_2) obtained from the Soxhlet extraction of EM and EM-R*X* (*X* = 0.001, 0.01, 0.02, 0.05, 0.2) microparticles. (b) Molecular-weight distribution of the soluble fraction of EM microparticles acquired from GPC measurements.

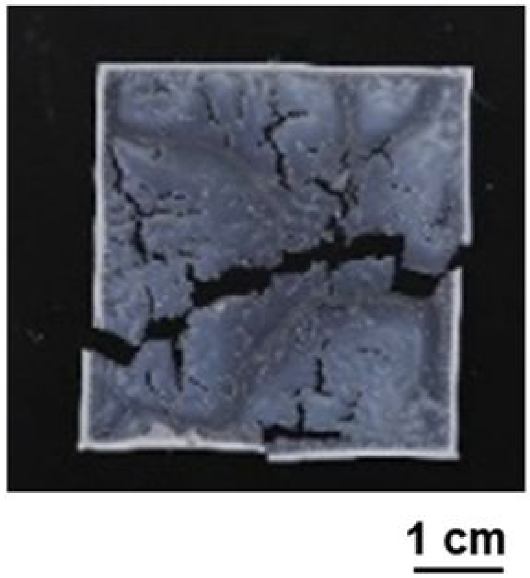

Figure S6. Photograph of a EM-R0.4 film. The EM-R0.4 microparticles formed a brittle film.

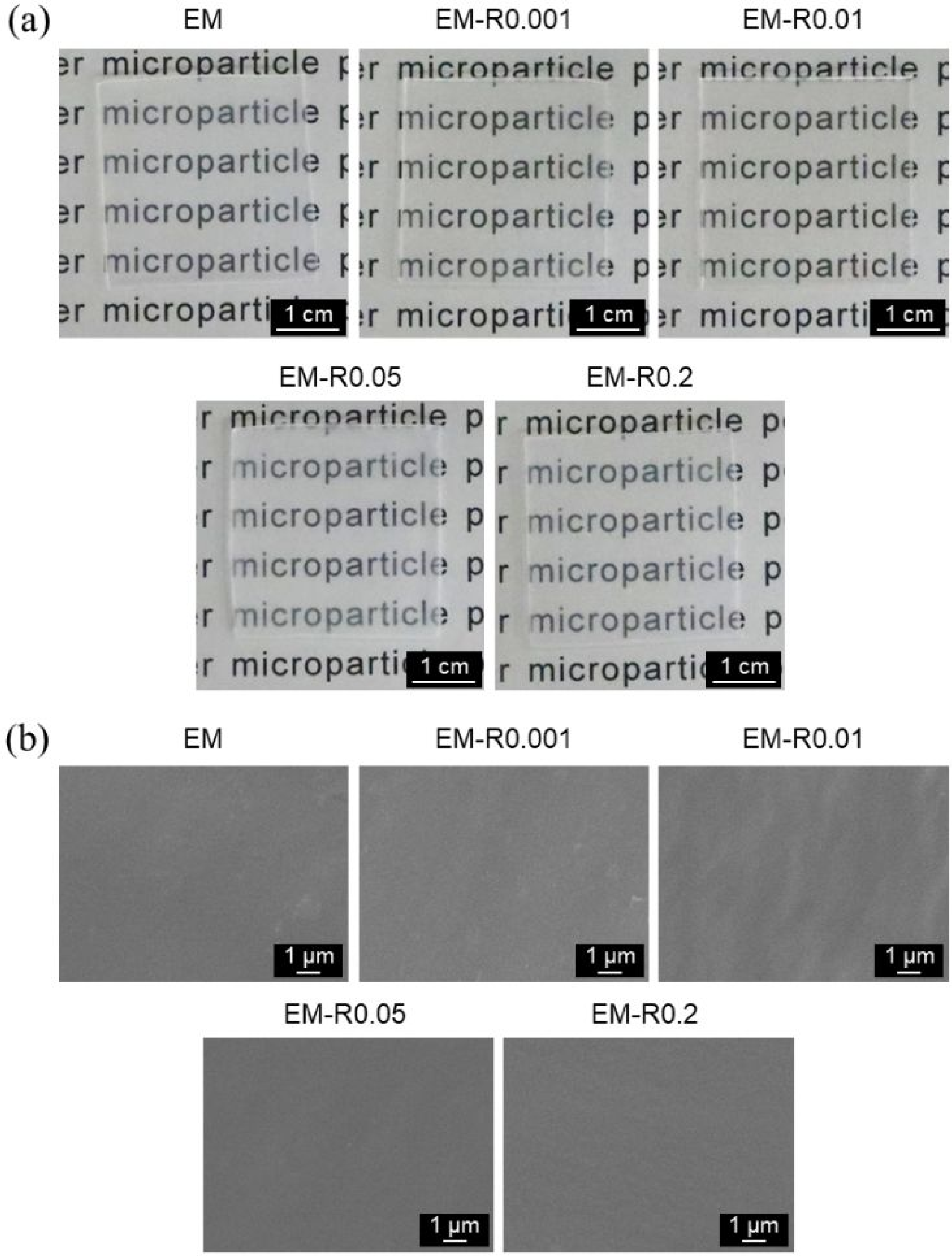

Figure S7. (a) Photographs and (b) SEM images (surface) of the EM and EM-R*X* (*X* = 0.001, 0.01, 0.05, 0.2) films.

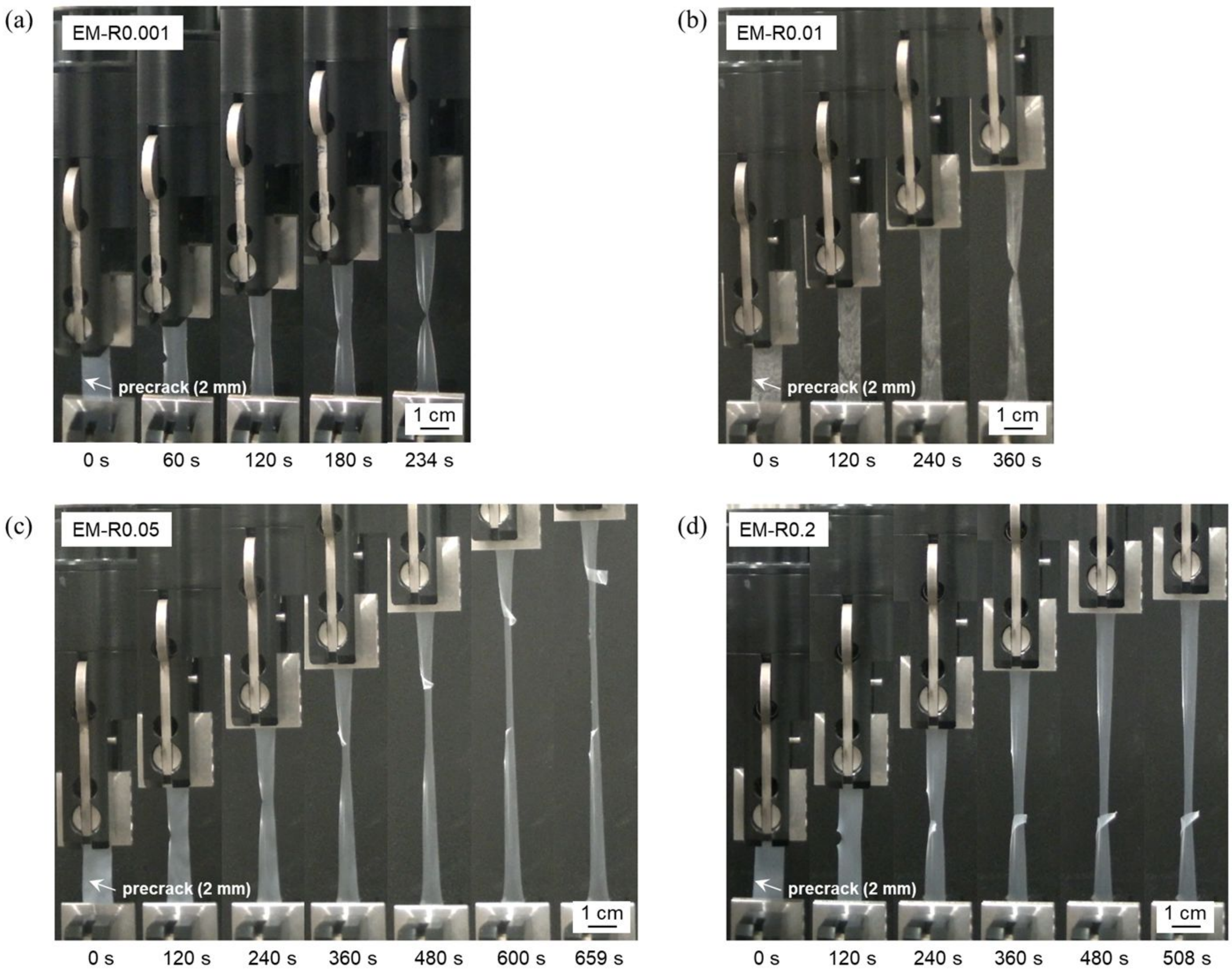

Figure S8. Time-lapse photographs the tear tests of the (a) EM-R0.001, (b) EM-R0.01, (c) EM-R0.05, and (d) EM-R0.2 films. The initial crack length *c* and elongation rate were fixed at 2 mm and 10 mm/min, respectively.

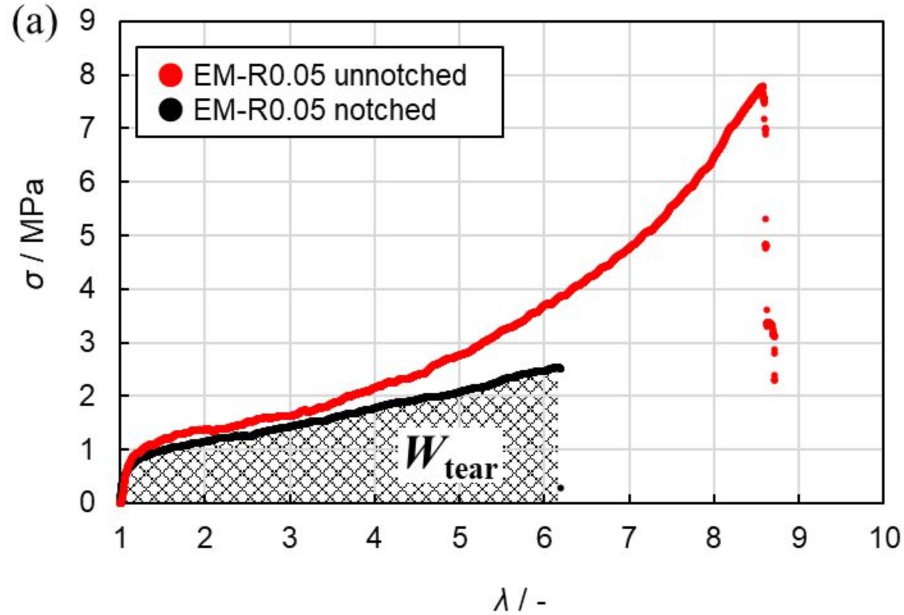

(b)

	Young's Modulus E / MPa	Maximum extension ratio λ_{max} / -	Maximum stress σ_{max} / -
notched	8.1 ± 1.4	5.8 ± 0.7	2.1 ± 0.4
unnotched	4.1 ± 2.7	8.5 ± 1.3	5.9 ± 2.1

Figure S9. (a) σ-λ curves for the notched and unnotched EM-R0.05 latex films. (b) The Young's modulus E, maximum extension ratio λ_{max}, and maximum stress σ_{max} values obtained from the σ-λ curves.

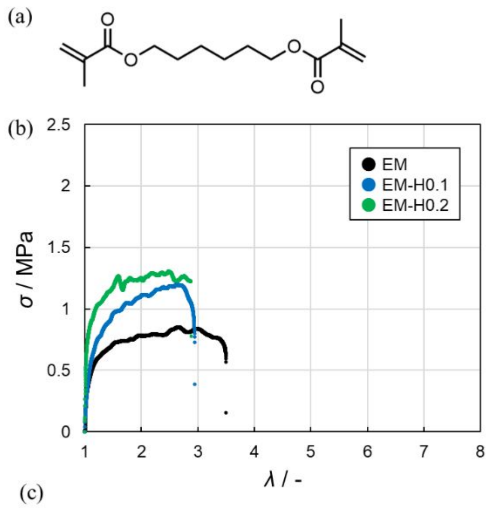

	W_{tear} / MJ m^{-3}	Young's Modulus E / MPa	λ_{max} / -	σ_{max} / -
EM	1.4±0.4	5.5±0.6	3.5±0.0	0.7 ±0.2
EM-H0.1	1.9±0.2	8.1±1.7	2.9±0.1	1.2 ±0.1
EM-H0.2	2.2±0.1	9.9±1.8	2.9±0.1	1.3 ±0.0

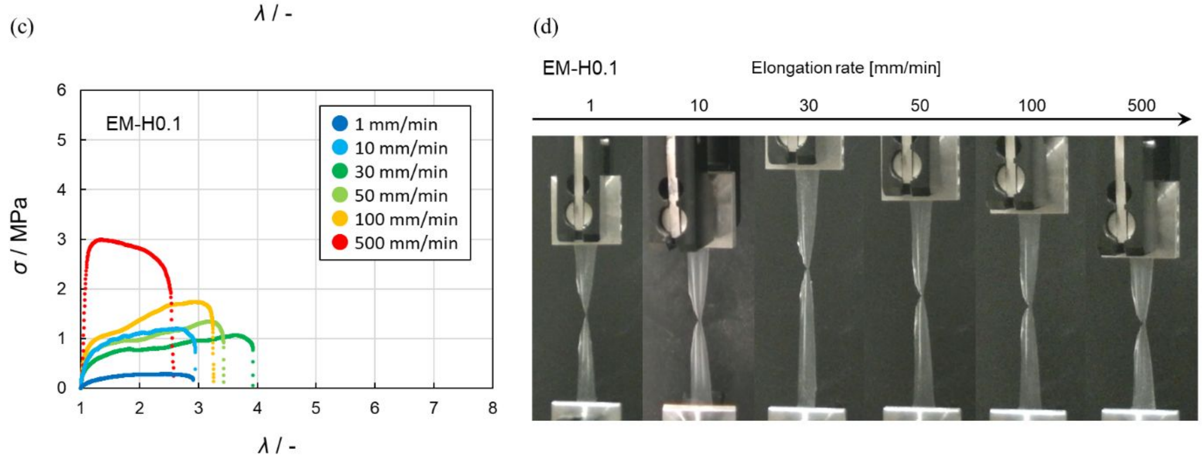

Figure S10. (a) Chemical structure of 1,6-hexanediol dimethacrylate (HDD), which was selected as a conventional chemical crosslinker. (b) Stress-extension ratio curves of tear tests for HDD-crosslinked EM-H films. Elongation rate was fixed at 10 mm/min. Elongation-rate dependence of (c) stress-extension ratio curves and (d) photographs of latex films just before fracture at various rates.

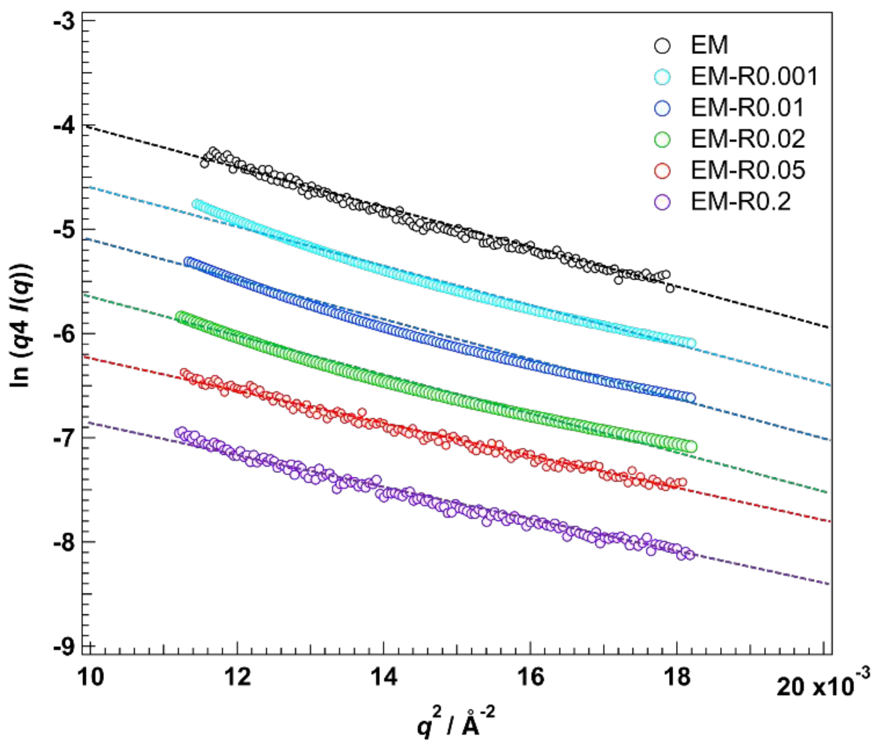

Figure S11. SAXS scattering intensity in the high-*q* range for EM and EM-R films.

(a)

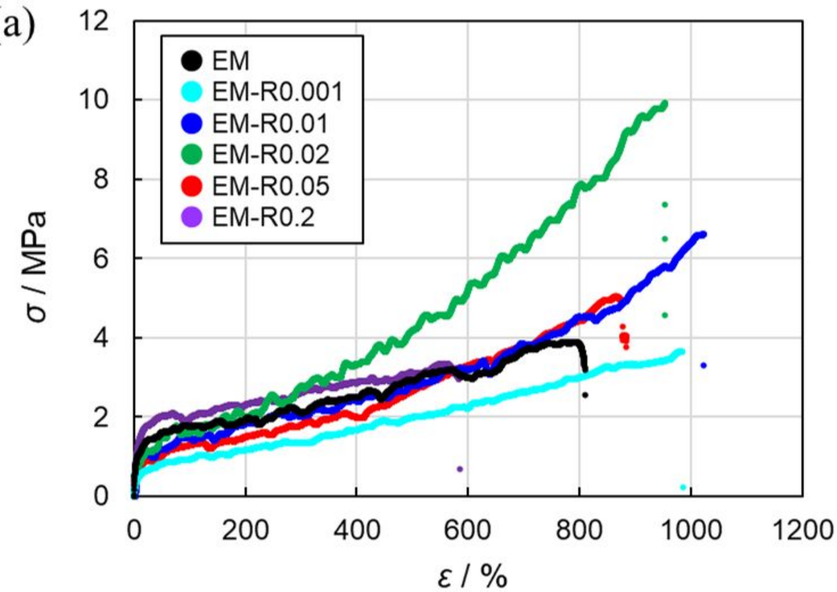

(b)

	Energy density function U / MJ m^{-3}	Young's modulus E / MPa	Maximum strain ε_{max} / %	Maximum stress σ_{max} / MPa
EM	16.9 ± 3.9	8.9 ± 6.6	789.3 ± 108.7	3.5 ± 0.6
EM-R0.001	19.4 ± 2.0	4.1 ± 2.3	959.2 ± 44.8	3.7 ± 0.2
EM-R0.01	34.4 ± 5.1	8.2 ± 2.4	932.3 ± 99.8	7.8 ± 1.5
EM-R0.02	43.3 ± 4.3	12.2 ± 1.2	954.3 ± 22.5	10.0 ± 1.3
EM-R0.05	23.3 ± 4.9	8.1 ± 3.1	925.6 ± 78.3	5.2 ± 0.6
EM-R0.2	14.9 ± 1.8	9.4 ± 14.7	592.2 ± 29.7	3.4 ± 0.5

Figure S12. (a) Stress-strain curves for the EM and EM-RX (X = 0.001, 0.01, 0.02, 0.05, 0.2) films obtained from tensile test measurements. (b) The Energy density function U, Young's modulus E, maximum strain ε_{max}, and maximum stress σ_{max} values obtained from the stress-strain curves. The tensile speed was fixed at 10 mm/min. Each curve was extracted from those close to its mean (N = 3).

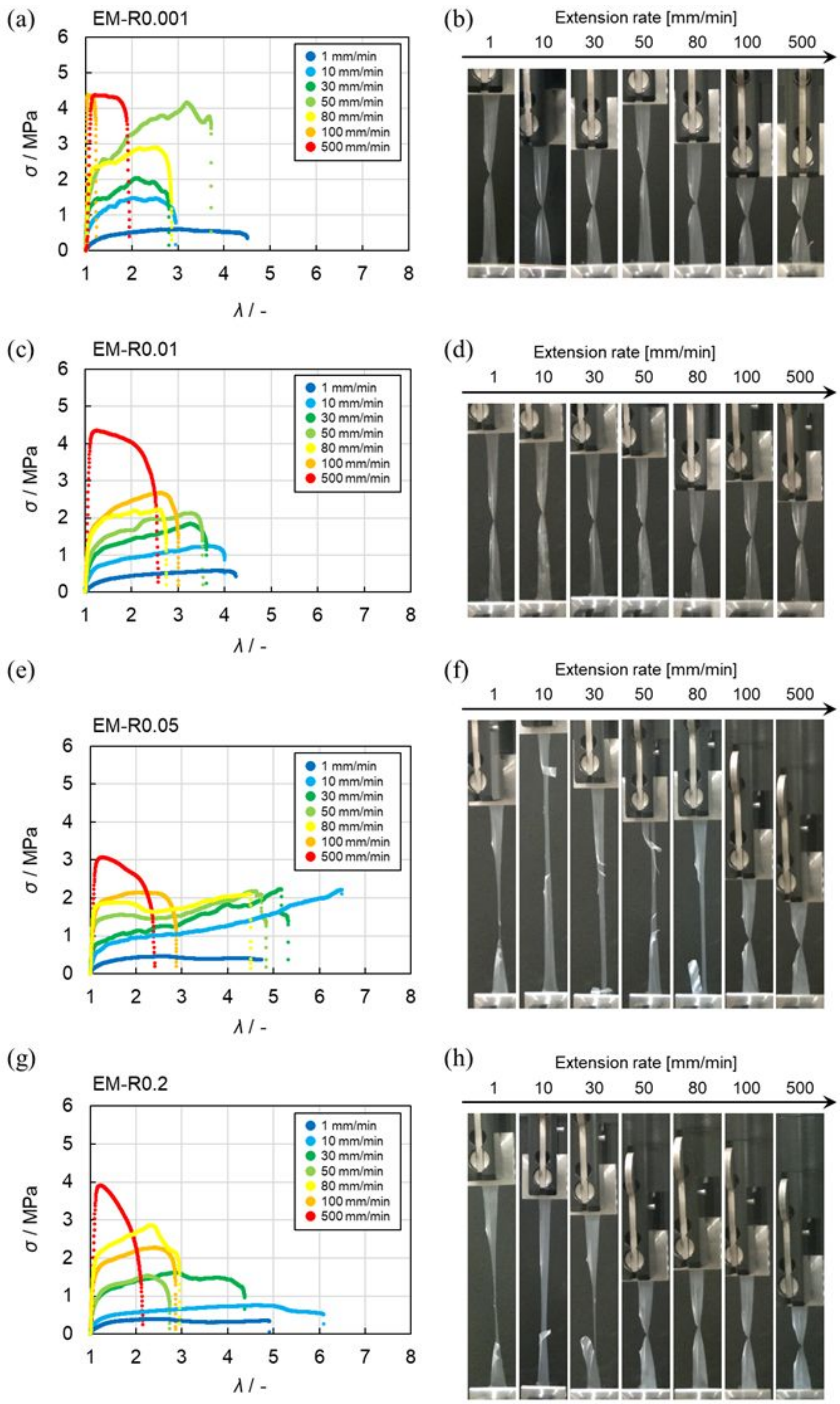

Figure S13. (a,c,e,g) Stress-extension ratio curves for the EM-R*X* latex films obtained from tear tests conducted at various elongation rates. (b,d,f,h) Photographs of the EM-R*X* latex films just before fracture at various elongation rates.

Movie S1. The fracture behavior of an EM film during a tear test at an elongation rate of 10 mm/min. Note that this video has been modified to 50x speed.

Movie S2. The fracture behavior of an EM-R0.02 film during a tear test at an elongation rate of 10 mm/min. Note that this video has been modified to 50x speed.